AIAA Aviation
22-26 June 2015, Dallas, TX
22nd AIAA Computational Fluid Dynamics Conference

Development of a Spectral-Element Approach for the Eikonal Equation

Scott M. Murman and Laslo T. Diosady*

NASA Ames Research Center, Moffett Field, CA, USA

Abstract

A novel spectral-element approach for the eikonal equation is presented based on the work of Tucker *et al.* This approach is readily implemented in standard finite-element flow solvers developed for the Navier-Stokes equations. Results are presented for distance function (level set) for three planar configurations: circular cylinder, NACA 0012 airfoil, and T106 airfoil. Results demonstrate that the approach is capable of arbitrary order of accuracy. For configurations with strong convex curvature, additional curvature-based dissipation is added to the eikonal equation to generate a weak solution consistent with the entropy condition.

1 Introduction

The eikonal equation

$$|\boldsymbol{\nabla} u| = f \tag{1}$$

$$u = g \quad \text{on } \Gamma \tag{2}$$

with f a known function with positive values, appears in many computational physics applications, including interface reinitialization[1–3], mesh generation[4–6], image segmentation[7,

*Science and Technology Corporation

8] and first-arrival travel times[9–11]. For example, when $f = 1$ and $g = 0$, then u is the distance function from the boundary Γ. Given this ubiquity, it is no surprise that there exist a number of efficient partial differential equation algorithms for solving the eikonal equation on Cartesian grids, for example the finite-difference Fast Marching[12, 13], Fast Sweeping[14, 15], and Group Marching[16] methods, along with finite-element Discontinuous-Galerkin methods[17].

While some of these methods can achieve $\mathcal{O}(N_V)$ complexity, where N_V is the number of volume degrees of freedom, there are still practical difficulties in their usage. In order to achieve efficiency these schemes make use of the hyperbolic nature of the eikonal equation, using specific sorting or sweeping through the volume combined with upwind schemes. This causality, along with the reliance upon a regular Cartesian lattice, makes the extension to general unstructured grids, or localized adaptation, problematic. For many applications higher-order methods are required, which for the above algorithms typically involves complex Essentially Non-oscillatory (ENO) schemes which are restricted to structured grids.

Hence, we see that these typical schemes for the eikonal equation require specialized algorithms, which are often difficult to implement efficiently in a parallel environment, and do not easily generalize to unstructured, high-order methods. Further, the solution of the eikonal equation is often complementary to a more significant physics simulation, and the data structures required may not be directly compatible between the two, necessitating a further complex post-processing step to transfer the solution.

An alternative is to sacrifice some formal algorithmic efficiency, and re-cast Eqn. 1 to more standard convection and diffusion operators, which can take advantage of existing infrastructure and algorithms to solve the resulting equation. For example, Tucker[18] developed a body-fitted, finite-volume formulation to calculate the distance from the wall for turbulence models, which leverages existing finite-volume solvers for the Navier-Stokes equations. This provides a direct path for an efficient parallel implementation that shares the same data structures as the primary Computational Fluid Dynamics (CFD) solver.

The objective of this work is to extend the philosophy of [18] to general unstructured, non-body-conforming meshes and high-order methods. Specifically, we seek to leverage our recent work on Discontinuous-Galerkin Spectral-Element methods for the Navier-Stokes equations[19–21] to develop an eikonal solver. This provides a parallel infrastructure which is arbitrary order of accuracy, and can handle general unstructured mesh topologies. The spectral-element method is implemented using an efficient three-dimensional tensor-product formulation. We've previously demonstrated that the cost of the residual evaluation using

this formulation can be made independent of order of accuracy through the use of software optimization[19]. Adding the eikonal equation to this infrastructure can enable multiphase or fluid-structure interaction simulations, by providing an efficient and accurate signed-distance function.

The current paper first covers the development of the method in a body-fitted spectral-element framework, then presents some "proof-of-concept" numerical experiments that demonstrate the performance of the approach. Some of the specific topics which require further research are discussed in the final Summary section.

2 Numerical Approach

Squaring the eikonal equation and writing the weak formulation we seek $u \in \mathcal{V}^p$, where $\mathcal{V}^p$ is a polynomial space, such that

$$(\boldsymbol{\nabla} u \cdot \boldsymbol{\nabla} u, v) = (f^2, v) \quad \forall v \in \mathcal{V}^p \tag{3}$$

Squaring the equation does come at a cost. The stiffness of the system is now increased, and it is not clear that the new system inherits the same boundedness properties as the original equation. Using integration by parts this is rewritten as

$$-(u\boldsymbol{\nabla} u, \boldsymbol{\nabla} v)_\Omega + \left(u\widehat{\boldsymbol{\nabla} u \cdot \boldsymbol{n}}, v\right)_{\partial\Omega} = (f^2, v)_\Omega + (u\boldsymbol{\nabla} \cdot \boldsymbol{\nabla} u, v)_\Omega \tag{4}$$

where the boundary curve is assumed to be a member of the set of element boundaries, $\Gamma \in \partial\Omega$, *i.e.* the mesh is boundary conforming. The overhat symbol, *e.g.* $u\widehat{\boldsymbol{\nabla} u \cdot \boldsymbol{n}}$, denotes the numerical flux function across the element boundary.

There are several options for solving Eqn. 4. One option is to require a high-order discretization ($N > 2$), and evaluate the curvature term $\boldsymbol{\nabla} \cdot \boldsymbol{\nabla} u$ directly. This has the advantage of solving a single scalar equation, but loses some formal accuracy, and was found to be too stiff for practical application due to the loss of accuracy in the curvature forcing term.

Another option is to introduce a scalar auxiliary variable for the curvature $\kappa = \boldsymbol{\nabla} \cdot \boldsymbol{\nabla} u$,

and construct a nonlinear system as

$$-\left(u\boldsymbol{\nabla}u,\boldsymbol{\nabla}v\right)_{\Omega}+\left(\widehat{u\boldsymbol{\nabla}u\cdot\boldsymbol{n}},v\right)_{\partial\Omega}=\left(f^{2},v\right)_{\Omega}+\left(u\kappa,v\right)_{\Omega} \tag{5}$$

$$-\left(\boldsymbol{\nabla}u,\boldsymbol{\nabla}\tau\right)_{\Omega}+\left(\widehat{\boldsymbol{\nabla}u\cdot\boldsymbol{n}},\tau\right)_{\partial\Omega}=\left(\kappa,\tau\right)_{\Omega} \tag{6}$$

$$u=g\quad\text{on }\Gamma \tag{7}$$

$$\boldsymbol{\nabla}u=f\boldsymbol{n}_{\Gamma}\quad\text{on }\Gamma \tag{8}$$

where $\boldsymbol{n}_{\Gamma}$ is the surface normal. This is a system of two scalar equations, however the boundary condition on $\boldsymbol{\nabla}u$ does not fully constrain the curvature κ. An auxiliary equation must be introduced to constrain the curvature, for example by specifying the curvature on the boundary Γ and using this to correct the computed curvature. This is similar to Li and Shu's Discontinuous-Galerkin least-squares approach for solving the Hamiltonian system, where the state must be constrained using the computed gradient and an auxiliary equation[22]. Given this complication, this approach was not pursued.

In the current work, an auxiliary variable is introduced for the gradient, $\boldsymbol{q}=\boldsymbol{\nabla}u$, resulting in a nonlinear system of equations,

$$-\left(u\boldsymbol{q},\boldsymbol{\nabla}v\right)_{\Omega}+\left(\widehat{u\boldsymbol{q}\cdot\boldsymbol{n}},v\right)_{\partial\Omega}=\left(f^{2},v\right)_{\Omega}+\left(u\boldsymbol{\nabla}\boldsymbol{q},v\right)_{\Omega} \tag{9}$$

$$-\left(u,\boldsymbol{\nabla}\tau\right)_{\Omega}+\left(\widehat{u\boldsymbol{n}},\tau\right)_{\partial\Omega}=\left(\boldsymbol{q},\tau\right)_{\Omega} \tag{10}$$

$$u=g\quad\text{on }\Gamma \tag{11}$$

$$\boldsymbol{q}=f\boldsymbol{n}_{\Gamma}\quad\text{on }\Gamma \tag{12}$$

Unlike the Local and Compact Discontinuous-Galerkin schemes[23, 24], the operator for the eikonal equation is quadratic, hence the equation for the gradient cannot be recombined back into the original equation.

Eqns. 9-10 form a forced hyperbolic system with eigenvalues, $\boldsymbol{\lambda}\cdot\boldsymbol{n}=\left(q_n\pm\sqrt{q_n^2+4u},0,0\right)$, where $q_n=\boldsymbol{q}\cdot\boldsymbol{n}$.* In the current Discontinuous-Galerkin framework, the numerical flux across the element boundaries must be supplied. Here a Lax upwind flux is used, *e.g.*

$$\left(\widehat{u\boldsymbol{q}\cdot\boldsymbol{n}},v\right)_{\partial\Omega}=\left(\left\{u\boldsymbol{q}\right\}\cdot\boldsymbol{n}-\frac{1}{2}\left|\boldsymbol{\lambda}\cdot\boldsymbol{n}\right|\left[\!\left[u\right]\!\right]\cdot\boldsymbol{n},v\right)_{\partial\Omega} \tag{13}$$

where $\{\phi\}$ and $[\![\phi]\!]$ are the average and jump operators respectively across the discontinuous

*The hyperbolic operator in isolation is singular, however the source terms add diagonal components to the system residual.

element boundary. Unfortunately, this straightforward implementation does not provide sufficient dissipation to maintain stability. When u is small $|\boldsymbol{\lambda}\cdot\boldsymbol{n}| \approx 2\,|q_n|$, however when the gradient is aligned with the element boundary this term is also small. This is especially troublesome when computing the distance from the boundary as the dissipation is typically most needed near the boundary where $u \downarrow 0$. To account for this a modified Lax upwind flux is employed,

$$\left(\widehat{u\boldsymbol{q}\cdot\boldsymbol{n}}, v\right)_{\partial\Omega} = \left(\{u\boldsymbol{q}\}\cdot\boldsymbol{n} - \frac{1}{2}\,|f|\,[\![u]\!], v\right)_{\partial\Omega} \tag{14}$$

where the absolute value on f is redundant.

Despite the numerical dissipation from the upwind flux, the discrete integration of Eqns. 9-10 is not guaranteed to converge to the weak solution which satisfies the entropy condition for the eikonal equation (*cf.* [25]). Dissipation is added by modifying the front-propagation speed to depend upon the curvature,

$$\boldsymbol{\nabla} u\cdot\boldsymbol{\nabla} u = f^2 + \epsilon\boldsymbol{\nabla}\cdot\boldsymbol{\nabla} u \tag{15}$$

where ϵ is a scalar, and $f^2 + \epsilon\boldsymbol{\nabla}\cdot\boldsymbol{\nabla} u > 0$. This is equivalent to modifying the front-propagation speed directly in Eqn. 1 and dropping terms proportional ϵ^2 after squaring the system. In the limit as $\epsilon \downarrow 0$, the entropy-satisfying solution for the original speed f is obtained.

Writing the weak formulation, and using integration by parts to transform the diffusion term Eqns. 9-10 become,

$$-(u\boldsymbol{q}, \boldsymbol{\nabla} v)_\Omega + \left(\widehat{u\boldsymbol{q}\cdot\boldsymbol{n}}, v\right)_{\partial\Omega} + (\epsilon\boldsymbol{\nabla} u, \boldsymbol{\nabla} v)_\Omega - \left(\epsilon\widehat{\boldsymbol{\nabla} u\cdot\boldsymbol{n}}, v\right)_{\partial\Omega} = (f^2, v)_\Omega + (u\boldsymbol{\nabla}\boldsymbol{q}, v)_\Omega \tag{16}$$

$$-(u, \boldsymbol{\nabla}\tau)_\Omega + (\widehat{u\boldsymbol{n}}, \tau)_{\partial\Omega} = (\boldsymbol{q}, \tau)_\Omega \tag{17}$$

$$u = g \quad \text{on } \Gamma \tag{18}$$

$$\boldsymbol{q} = f\boldsymbol{n}_\Gamma \quad \text{on } \Gamma \tag{19}$$

The diffusion in Eqn. 16 is applied directly using the gradient of the state rather than $\boldsymbol{q}$ to better remove oscillations during transient start-ups. The numerical flux of Bassi and Rebay[26] is used for the diffusion term across a discontinuous boundary.

The original eikonal equation has been transformed from a scalar hyperbolic equation to a system of mixed hyperbolic elliptic equations. At first this does not seem to be progress, however the system Eqns. 16-17 is easily implemented within the parallel Discontinuous-Galerkin spectral-element infrastructure described previously. The same matrix-free, tensor-product

sum-factorization approach is used, along with optimized kernels using SIMD vectorization. Further, it is straightforward to extend the tensor-product Alternating Direction Implicit (ADI) preconditioner described in [19] to the current system using the spectral decomposition of the hyperbolic operators.

3 Numerical Experiments

The system for the stationary eikonal equation, Eqns. 16-17, is computed on an unstructured mesh with hexahedral elements. The numerical examples here use planar geometry as an initial proof-of-concept, though the implementation and computed solution are three-dimensional. The finite-element mesh is generated using an iso-parametric mapping of rational interpolants which enables us to evaluate the geometry information at spectral accuracy. The geometry of the mesh is represented using the same polynomial order as the computed solution. All of the examples compute the distance function from the boundary Γ, *i.e.* $f = 1$ and $g = 0$. The outer boundaries of the computational domain use a Neumann boundary condition $\boldsymbol{\nabla} u \cdot \boldsymbol{n} = 0$.

The system rapidly converges when the initial guess is "close" to the final solution, however with general initial conditions the system becomes difficult to converge as isolated non-physical pockets ($u < 0$) develop and persist. To alleviate this problem, the solution is initially computed with a relatively large value of the diffusion coefficient $\epsilon \sim \mathcal{O}(1)$, essentially rendering Eqn. 16 Poisson's equation. This initializes the field with a smooth distance function based on the prescribed boundary conditions. As the elliptic system satisfies the maximum principle, the distance everywhere is guaranteed to be positive. From this the diffusion coefficient is reduced, and the convergence is well behaved. It is not claimed this *ad-hoc* procedure is optimal, or even desirable, however it is effective is demonstrating the performance of the approach. The solution at higher orders is initialized by projecting the converged solution from lower order in a spectral continuation manner, without manipulating the diffusion.

The formal accuracy of the scheme is verified by computing the distance from a circular cylinder, for which the exact solution is readily available. The convergence of the residual is presented in Fig. 1a. As described above, the dissipation is incrementally reduced to zero using the $N = 2$ polynomial basis, where N is the solution order. This eventually converges to roughly machine epsilon. The progressively higher-order solutions are initialized and rapidly converge again to roughly machine epsilon. The computed error with progressively

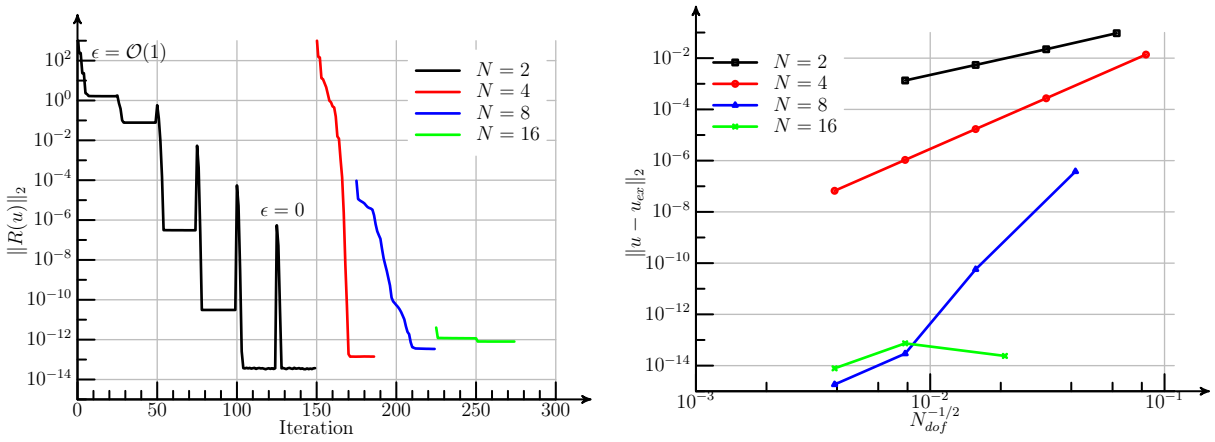

(a) Convergence **(b)** Error

Figure 1: Solution of the distance function about a circular cylinder.

finer resolution is presented in Fig. 1b. All schemes demonstrate formal accuracy in the asymptotic limit. The error in the solution at $N = 16$ on the coarsest resolution available is already machine epsilon. Figure 1b highlights the benefits of higher-order for this application, as the same error level is achieved using orders of magnitude fewer degrees of freedom with the higher-order polynomial basis.

The utility of the scheme is tested for two airfoil configurations: the NACA 0012 which contains a sharp trailing edge, and the T106 configuration which combines regions of both convex and concave curvature. Unlike the circular cylinder configuration, here the residual does not converge to near machine epsilon. These cases converge several orders of magnitude before stalling. Similarly, it is not possible to reduce the auxiliary dissipation coefficient, ϵ, to zero and still generate physically-consistent results.

The solution of Eqns. 16-17 on the NACA 0012 for 2nd-, 4th-, and 8th-order accuracy is presented in Fig. 2. In these tests the resolution itself is increasing, *i.e.* the number of degrees of freedom is not held fixed. The contours show the distance field $u \in [0, 2c]$. As expected, with the non-zero dissipation in regions of strong concave curvature near the leading and trailing edges the marching of the distance field is strongly retarded. As the solution order increases the resolution of the curvature increases outside the region of influence of the dissipation, however near the body $\epsilon \sim u$, and the dissipation term still dominates.

Similar solutions at 2nd-, 4th-, and 8th-order accuracy for the T106 airfoil are presented in Fig. 3. Again, as expected, near the leading and trailing edges the marching of the distance field is strongly retarded, while the opposite occurs in the region of convex curvature.

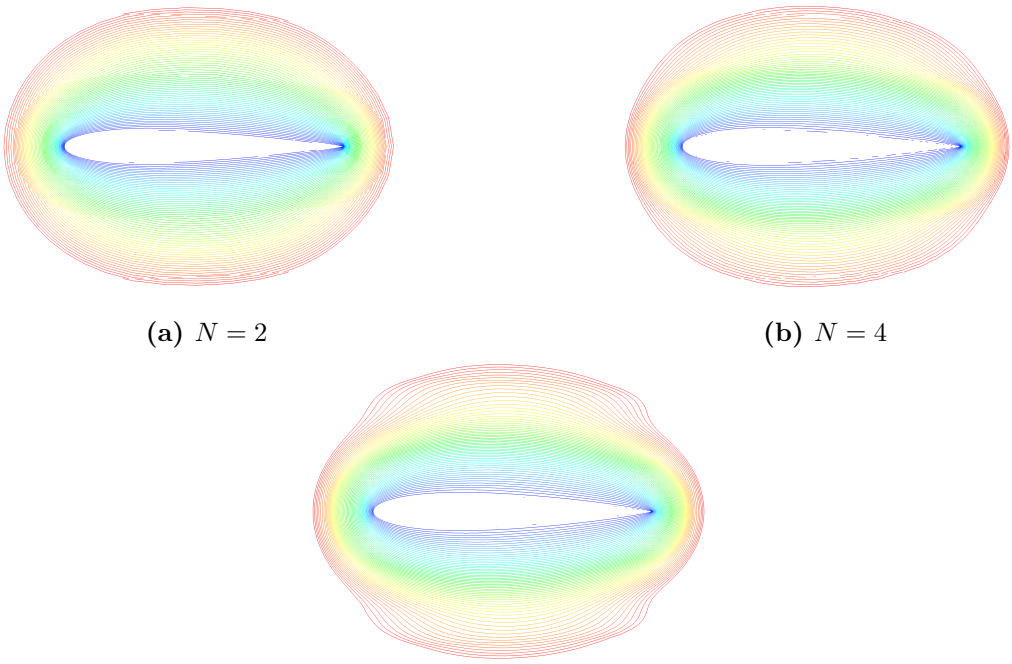

(a) $N = 2$ **(b)** $N = 4$

(c) $N = 8$

Figure 2: Solution of the distance function about a NACA 0012 airfoil. $u \in [0, 2c]$.

This prevents the lines of constant distance crossing, *i.e.* generates a weak solution consistent with entropy condition. In this configuration it is noticed that the region outside the strong influence of the auxiliary dissipation, *i.e.* when $u > \epsilon$, the solution starts to develop oscillations as the order increases. This is evidence that the auxiliary dissipation is not simply directing the solution to satisfy the entropy condition, but is also an *ad-hoc* method of stabilization. If the level sets are not constant curvature when the effective dissipation is removed, as is the case here in the T106 airfoil configuration, oscillations appear.

4 Summary

A novel spectral-element approach for the eikonal equation is presented. This approach is readily implemented in standard flow solvers developed for the Navier-Stokes equations. Verification results on a circular cylinder demonstrate that the approach is capable of essentially arbitrary order of accuracy, however there are several issues still outstanding. Currently the convergence is limited on practical problems. This is due in part to not including the source terms in the ADI preconditioner. This is a topic which will be visited in future work. Sim-

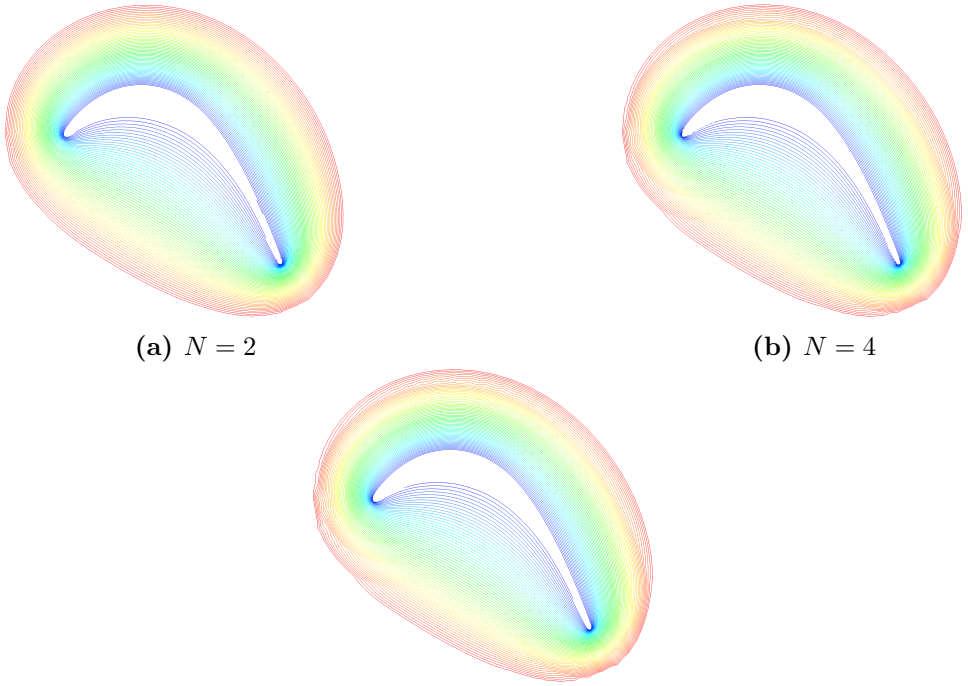

(a) $N = 2$ **(b)** $N = 4$

(c) $N = 8$

Figure 3: Solution of the distance function about a T106 airfoil. $u \in [0, c]$.

ilarly, the globalization procedure currently being used (*cf.* [27]) is incompatible with the eikonal system, hence a robust solution of the nonlinear system is not possible. This topic will also be investigated going forward. It is important to understand that solving these issues improves the robustness of the method for other systems of equations, such as when using Reynolds-averaged Navier-Stokes (RANS) turbulence models, which also have general source terms. This is part of the motivation to re-use the same infrastructure as the original CFD solver when solving the eikonal system.

Specific to the eikonal equation, the numerical scheme does not inherently reproduce the physical entropy solution to the original system. This necessitates the addition of *ad-hoc* dissipation in order to produce a consistent solution. While this is representative of the current state-of-the-art for solving the stationary eikonal system, it is still unpleasant. Further analysis is required in order to understand and robustly produce a physically-consistent solution without requiring *ad-hoc* procedues.

References

[1] Sussman, M., Smereka, P., and Osher, S., "A Level Set Approach for Computing Solutions to Incompressible Two-Phase Flow," *Journal of Computational Physics*, vol. 114, pp. 146–159, 1994.

[2] Peng, D., Merriman, B., Osher, S., Zhao, H., and Kang, M., "A PDE-Based Fast Local Level Set Method," *Journal of Computational Physics*, vol. 155, pp. 410–438, 199.

[3] Chopp, D.L., "Some improvements of the fast marching method," *SIAM Journal of Scientific Computing*, vol. 23, no. 1, pp. 230–244, 2001.

[4] Bagnerini, P., Hoch, P., and Rascle, "The Eikonal Equation on a Manifold. Applications to Grid Generation or Refinement," in *Hyperbolic Problems: Theory, Numerics, Applications*, vol. 140, pp. 109–118, Birkhäuser Basel, 2001.

[5] Wang, Y., Guibault, F., and Camarero, R., "Automatic Near-Body Domain Decomposition Using the Eikonal Equation," in *Proceedings of the 14th International Meshing Roundtable*, pp. 91–107, 2005.

[6] Perrson, P.O., "Mesh Generation for Implicit Geometries," Master's thesis, Massachusetts Institute of Technology, 2005.

[7] Sofou, A. and Maragos, P., "PDE-Based Modeling of Image Segmentation using Volumic Flooding," in *Proceedings of International Conference on Image Processing*, pp. 431–434, 2003.

[8] Alvino, C., Unal, G., Slabaugh, G., Peny, B., and Fang, T., "Efficient segmentation based on Eikonal and diffusion equations," *International Journal of Computer Mathematics*, vol. 84, no. 0, pp. 1309–1324, 2007.

[9] Mo, L-W and Harriss, J. M., "Finite-Difference calculation of direct-arrival traveltimes using the eikonal equation," *Geophysics*, vol. 67, no. 4, pp. 1270–1274, 2002.

[10] Taillandier, C., Noble, M., Chauris, H., and Calandra, H., "First-arrival traveltime tomography based on the adjoint-state method," *Geophysics*, vol. 74, no. 6, pp. 57–66, 2009.

[11] Lan, H. and Zhang, Z., "A High-Order Fast-Sweeping Scheme for Calculating First-Arrival Travel Times with an Irregular Surface," *Bulletin of the Seismological Society of America*, vol. 103, no. 3, pp. 2070–2082, 2013.

[12] Tsitsiklis, J.N., "Efficient Algorithms for Globally Optimal Trajectories," *IEEE Transactions on Automatic Control*, vol. 40, pp. 1528–1538, 1995.

[13] Sethian, J.A., "A Fast Marching Level Set Method for Monotonically Advancing Fronts," *Proceedings of the National Academy of Sciences*, vol. 93, no. 4, pp. 1591–1595, 1996.

[14] Zhao, H., "A Fast Sweeping Method for Eikonal Equations," *Mathematics of Computation*, vol. 74, no. 250, pp. 603–627, 2004.

[15] Detrixhe, M., Gibou, F., and Min, C., "A Parallel Fast Sweeping Method for Eikonal Equations," *Journal of Computational Physics*, vol. 237, pp. 46–65, 2013.

[16] Kim, S., "A $\mathcal{O}(\mathcal{N})$ Level Set Method for Eikonal Equations," *SIAM Journal on Scientific Computing*, vol. 22, no. 6, pp. 2178–2193, 2001.

[17] Zhang, Y-T, Chen, S., Li, F., Zhao, H., and Shu, C-W, "Uniformly accurate discontinuous Galerkin fast sweeping methods for Eikonal equations," *SIAM Journal on Scientific Computing*, vol. 33, no. 4, pp. 1973–1896, 2011.

[18] Tucker, P.G., "Differential equation-based wall distance computation for DES and RANS," *Journal of Computational Physics*, vol. 190, no. 1, pp. 229–248, 2003.

[19] L. Diosady and S. Murman, "Design of a Variational Multiscale Method for Turbulent Compressible Flows," AIAA Paper 2013-2870, June 2013.

[20] L. Diosady and S. Murman, "DNS of Flows over Periodic Hills using a Discontinuous Galerkin Spectral-Element Method," AIAA Paper 2014-2784, June 2014.

[21] L. Diosady and S. Murman, "Higher-Order Methods for Compressible Turbulent Flows Using Entropy Variables," AIAA Paper 2105-0294, 2015.

[22] Li, F. and Shu, C-W., "Reinterpretation and simplified implementation of a discontinuous Galerkin method for Hamilton-Jacobi equations," *Applied Mathematics Letters*, vol. 18, no. 11, pp. 1204–1209, 2005.

[23] Cockburn, B. and Shu, C.-W., "The Local Discontinuous Galerkin Method for Time-Dependent Convection-Diffusion Systems," *Siam Journal on Numerical Analysis*, vol. 35, no. 6, pp. 2440–2463, 1998.

[24] Peraire, J. and Persson, P.-O., "The Compact Discontinuous Galerkin (CDG) Method for Elliptic Problems," *SIAM Journal on Scientific Computing*, vol. 30, no. 4, pp. 1806–1824, 2008.

[25] Sethian, J.A., "Theory, algorithms, and applications of level set methods for propagating interfaces," *Acta Numerica*, vol. 5, pp. 309–395, 1996.

[26] Bassi, F. and Rebay, S., "A high-order accurate discontinuous finite element method foro the numerical solution of the compressible Navier-Stokes equations," *Journal of Computational Physics*, vol. 131, no. 2, pp. 267–279, 1997.

[27] Ceze, M. and Murman, S.M., "Global Convergence Strategies for a Spectral-Element Space-Time Discontinuous-Galerkin Discretization of the Navier-Stokes Equations," in *27th International Conference on Parallel Computational Fluid Dynamics*, 2015.